Cell Research (2009) 19:651-664.

www.nature.com/cr

ORIGINAL ARTICLE

Temporal and spatial profiling of nuclei-associated proteins upon TNF-α/NF-κB signaling

Dan-jun Ma[1], Su-Jun Li[1], Lian-Shui Wang[1], Jie Dai[1], Shi-lin Zhao[1], Rong Zeng[1]

[1]*Key Laboratory of Systems Biology, Institute of Biochemistry and Cell Biology, Shanghai Institutes for Biological Sciences, Chinese Academy of Sciences, Shanghai, 200031, China*

The tumor necrosis factor (TNF)-α/NF-κB-signaling pathway plays a pivotal role in various processes including apoptosis, cellular differentiation, host defense, inflammation, autoimmunity and organogenesis. The complexity of the TNF-α/NF-κB signaling is in part due to the dynamic protein behaviors of key players in this pathway. In this present work, a dynamic and global view of the signaling components in the nucleus at the early stages of TNF-α/NF-κB signaling was obtained in HEK293 cells, by a combination of subcellular fractionation and stable isotope labeling by amino acids in cell culture (SILAC). The dynamic profile patterns of 547 TNF-α-induced nuclei-associated proteins were quantified in our studies. The functional characters of all the profiles were further analyzed using that Kyoto Encyclopedia of Genes and Genomes (KEGG) pathway annotation. Additionally, many previously unknown effectors of TNF-α/NF-κB signaling were identified, quantified and clustered into differential activation profiles. Interestingly, levels of Fanconi anemia group D2 protein (FANCD2), one of the Fanconi anemia family proteins, was found to be increased in the nucleus by SILAC quantitation upon TNF-α stimulation, which was further verified by western blotting and immunofluorescence analysis. This indicates that FANCD2 might be involved in TNF-α/NF-κB signaling through its accumulation in the nucleus. In summary, the combination of subcellular proteomics with quantitative analysis not only allowed for a dissection of the nuclear TNF-α/NF-κB-signaling pathway, but also provided a systematic strategy for monitoring temporal and spatial changes in cell signaling.

***Keywords*:** quantitative analysis, SILAC, proteomics, TNF-α/NF-κB, nucleus, FANCD2, subcellular fractionation

Cell Research (2009) **19**:651-664. doi: 10.1038/cr.2009.46; published 28 April 2009

Introduction

Members of the tumor necrosis factor (TNF) ligand family mediate signals involved in numerous biological processes including apoptosis, cellular differentiation, host defense, inflammation, autoimmunity and organogenesis. As shown in recent studies, they can affect pathogenesis of several diseases, including cancer, arthritis, septic shock and inflammatory disease [1-3]. The pro-inflammatory cytokine TNF-α is believed to be an important trigger in TNF-α/NF-κB-signaling pathway. It leads to the activation of the transcription factor NF-κB. NF-κB activity is controlled by signal-induced degradation of inhibitors (IκB-α, -β and -ε) that bind to NF-κB, preventing its nuclear translocation. The signal in the TNF-α/NF-κB pathway is transduced to the IκB kinase complex upon the exposure of cells to TNF-α stimulation, leading to the rapid phosphorylation, ubiquitination and proteolytic degradation of each IκB isoform. This allows NF-κB to translocate to the nucleus and regulate transcription [2, 4].

Previous studies have functionally characterized the protein components of the TNF-α/NF-κB-signaling pathway by classic molecular biology and cell biology methods [5-7]. Using mass-spectrometry-based proteomics and SILAC method [8, 9], it is possible to delineate the global events of a signaling pathway. Several signaling pathways including those of EGF, FGF, Wnt, interferon-

Correspondence: Rong Zeng
E-mail: zr@sibs.ac.cn

Abbreviations: TNF (tumor necrosis factor); SILAC (stable isotope labeling by amino acids in cell culture); LC-MS/MS (liquid chromatography tandem mass spectrometry); LTQ-Orbitrap (linear ion trap/Orbitrap); HPRD (Human Protein Reference Database); SMARC (SWI/SNF-related matrix-associated actin-dependent regulator chromatin); KEGG (Kyoto Encyclopedia of Genes and Genomes)

Received 17 September 2008; revised 8 October 2008; accepted 9 October 2008; published 28 April 2009

alpha, insulin and TGF-β, have been systematically analyzed by this mass-spectrometry-based proteomics method [10-15]. These studies facilitate functional characterization of protein complexes and signaling pathways, and help to provide a more global understanding of those complicated biological processes.

Of course, the complexity of signaling is caused not only by the involvement of numerous proteins, but also by the dynamic protein behavior in cellular compartment. Many proteins are often observed to dynamically shuttle between cellular compartments, for example NF-κB (nucleocytoplasmic shuttling). These shuttling mechanisms are required for signaling pathways to respond properly to cytokines [16]. The cytokine-induced nuclear import and export of signaling proteins have been shown to be essential in various biological systems [17, 18]. Therefore, the nuclear function of various proteins is critical to TNF-α/NF-κB signaling.

Here, we investigated the dynamic behaviors of nuclear proteins upon stimulation with TNF-α in HEK293 cells by using SILAC in combination with subcellular fractionation and liquid chromatography tandem mass spectrometry (LC-MS/MS) analysis. The obtained results should help improve our understanding of both the temporal and spatial characteristics of the TNF-α/NF-κB signaling pathway.

Results

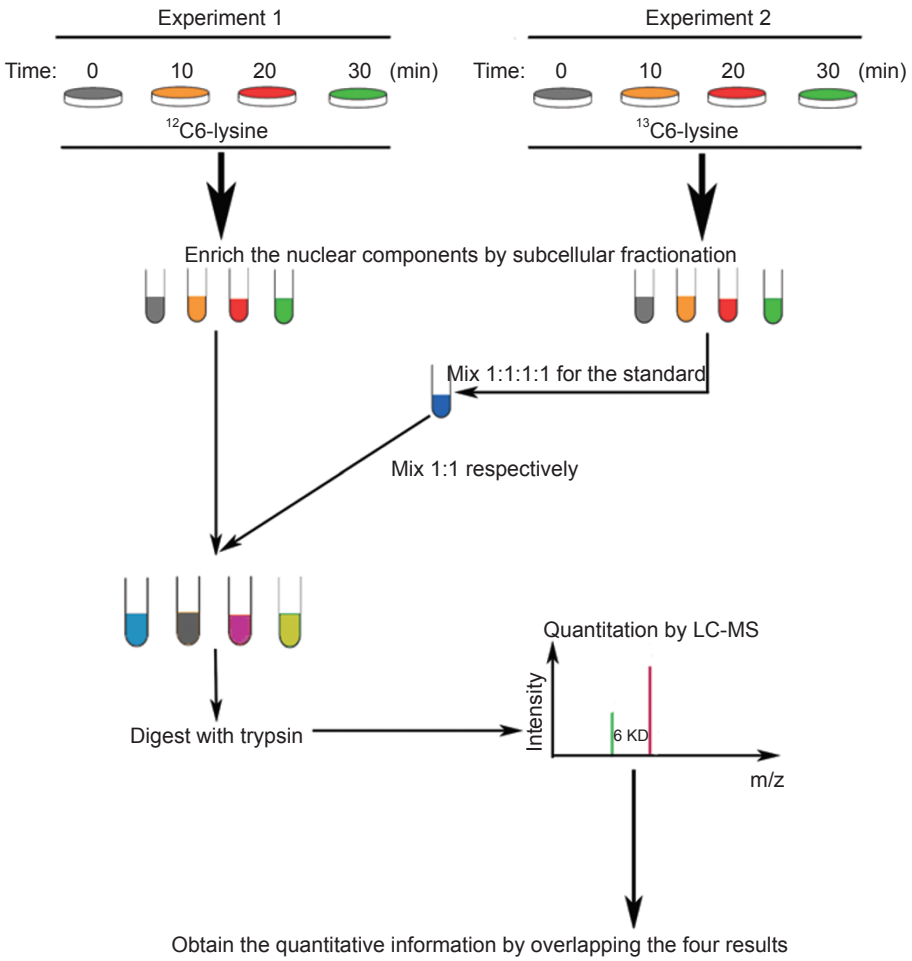

Figure 1 The flowchart of the quantitative analysis of nuclei-associated proteins upon TNF-α stimulation. HEK293 cells were grown in the light medium substituted with ^{12}C6-lysine and in the heavy medium substituted with ^{13}C6-lysine. These cell populations were stimulated with TNF-α for 0 min, 10 min, 20 min or 30 min, and subsequently submitted to subcellular fractionation. Equal amounts of the 'heavy' nuclear fractions were combined as a standard. After the four 'light' nuclear fractions were equally mixed with the standard and digested by trypsin, these samples were analyzed by LC-MS/MS. The SILAC results of the nuclei-associated proteins upon TNF-α stimulation were obtained by analyzing the quantitative information in samples from the four time points.

Quantitative analysis of nuclei-associated proteins upon TNF-α stimulation

Here, we used SILAC to generate a global and dynamic view of nuclei-associated proteins in TNF-α-dependent signaling. The methodology used is shown in Figure 1. Briefly, HEK293 cell populations were grown in light medium supplemented with ^{12}C6-lysine or in heavy medium supplemented with ^{13}C6-lysine. After the complete incorporation with the light or heavy SILAC amino acids, the cell populations were stimulated with TNF-α for 0 min, 10 min, 20 min or 30 min and were then collected and subjected to subcellular fractionation. Stepwise extraction of cytosolic fraction, organelle/membrane fraction, nuclear fraction and cytoskeletal fraction was performed using the subcellular proteome extraction kit. As expected, Lamin B1 was enriched in the nuclear fraction, while HSP90 showed the contrary pattern (Supplementary information, Figure S1A).

To validate the response to TNF-α stimulation in our experiments, P65 and IκBα protein levels were analyzed by western blotting (Figure 2A). P65 was increased in the nucleus and decreased in the cytoplasm upon stimulation [19]. Further, cytoplasmic IκBα was decreased upon stimulation [4]. GAPDH, the housekeeping protein, remained almost unchanged following TNF-α addition [20]. These results were as expected, indicating that our cell culture model is responsive to TNF-α signaling.

Equal amounts of 'heavy' nuclear fractions were combined as a standard. Such a standard can comprise more proteins than each fraction. Therefore, this would enable quantifying more proteins with SILAC results. After equally mixing the four 'light' nuclear fractions with such standards and digesting with trypsin, these samples were subjected to mass spectrometry analysis (see Materials and Methods). In total, 2 718 protein groups (7 567 unique peptides) were characterized in the 0 min fraction, 2 897 protein groups (8 911 unique peptides) in the 10 min fraction, 2 306 protein groups (7 135 unique peptides) in the 20 min fraction and 2 674 protein groups (7 728 unique peptides) in the 30 min fraction (Supplementary information, Table S1). In addition, over 70% of these proteins were identified in at least two fractions and 47% in at least three fractions (data not shown). This implied a good level of reproducibility in these assays.

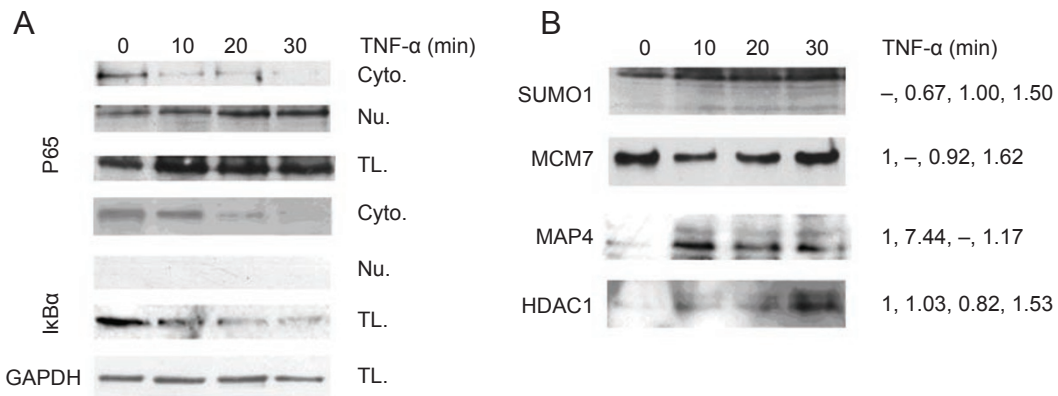

Figure 2 Western blotting verification of selected proteins. **(A)** The validation of the response to the stimulation with TNF-α by western blotting. P65 was increased in the nucleus and reduced in the cytoplasm upon stimulation. IκBα was reduced upon stimulation. GAPDH, the housekeeping gene, remained almost unchanged under such conditions. **(B)** The validation of SILAC ratios by western blotting. SILAC ratios of individual proteins are indicated. These results were well consistent with the western blotting analysis on these four proteins. Cyto., cytoplasmic fraction; Nu., nuclear fraction; TL., total cell lysates.

Table 1 Peptides and proteins identified and quantitated in the nuclear fractions

Fraction	Unique peptides	Total peptides	Protein groups	Proteins	Proteins_R[1]
0 min[2]	7567	40317	2718	5892	1584
10 min[2]	8911	58563	2897	6339	1464
20 min[2]	7135	56056	2306	5012	1007
30 min[2]	7728	40525	2674	5703	1378

[1]'Proteins_R' stands for proteins with SILAC ratio in this experiment.
[2]Combined cell samples stimulated with TNF-α for 0 min, 10 min, 20 min or 30 min with the standard.

As illustrated in Figure 1, the resulting mass spectrum will show distributions of isotopic ratios between the 'heavy' and 'light' peptide pairs. Therefore, quantitation of the relative changes of the labeled peptides is possible by comparison of their intensities in the mass spectrum. In our study, there were 1 584, 1 464, 1 007 and 1 378 proteins obtained with SILAC results in the 0 min fraction, 10 min fraction, 20 min fraction and 30 min fraction, respectively (Table 1).

All identified proteins from our MS analyses (including those with and without SILAC results) were searched against the Swiss-Prot database for subcellular annotations. Among those with annotations, more than 50% were annotated as nuclear proteins (Supplementary information, Figure S1B). Therefore, our fractionation could be considered as good quality nuclear fractionation [21, 22].

Preprocessing and validation of the quantitative data

All SILAC results of proteins were normalized using their labeled peptide ratio (Ratio=Total Peptide $hits_{light}$/ Total Peptide $hits_{heavy}$) in each fraction (see see Materials and Methods). Supplementary information, Figure S2A shows that these normalized results were more symmetric and normal in holistic approach compared to the raw SILAC results. After normalization, the distribution of the fold changes of all the quantitated proteins displayed an almost symmetrical pattern in all the three fractions (Figure 3). 'Housekeeping' proteins such as Lamin, ribonucleoproteins and nuclear pore complex proteins were found to have fold changes less than 1.28 in our results compared with 0 min time point (Supplementary information, Table S2). This indicated the SILAC results could measure changes in protein levels in our study.

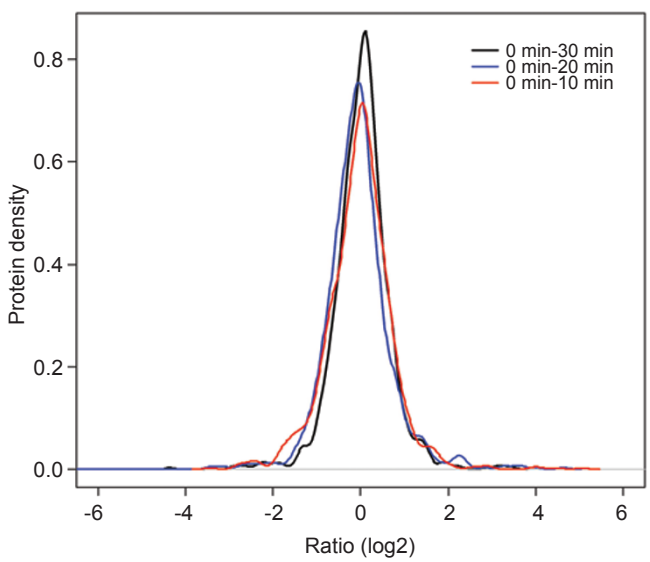

Figure 3 The distribution of fold changes in all quantitative proteins. The protein fold changes at the 10 min, 20 min and 30 min time point were calculated by comparison to the 0 min time point, and transformed into the log scale (base 2) after preprocessing. The distribution of the fold changes of all the quantitated proteins displayed an almost symmetrical pattern in each fraction. The ratios of 0 min to 10 min, 0 min to 20 min and 0 min to 30 min are indicated by red, blue and black lines, respectively.

The relative standard deviation (%SD) of all the proteins in different fractions showed a quantitation precision better than 15% (Supplementary information, Figure S2B) [23]. Therefore, 1.5 was chosen as the conservative threshold for a significant ratio change during TNF-α stimulation in the present study. On the basis of this criterion, the number of changed proteins was 235, 130 and 155 during the period between 0-10 min, 10-20 min and 20-30 min, respectively (data not shown). Almost 13% of proteins with SILAC results showed significant changes in our study. This is consistent with previous work [15, 24].

To further confirm these SILAC results, four proteins were analyzed by western blotting. Upon TNF-α stimulation, the levels of SUMO1 and HDAC1 increased over the 30 min time course. Mini-chromosome maintenance protein 7 (MCM7) showed an immediate decrease at the 10 min point, then it was increased to the almost basal level, whereas MAP4 showed an opposite trend (Figure 2B). As shown in Figure 2B, the SILAC results were well consistent with the western blotting analysis on these four proteins. Therefore, our strategy, which combined SILAC and high-resolution mass spectrometry, is a reliable approach to generate a panel of differential proteins during TNF-α/NF-κB signaling.

Temporal profile patterns reveal different categories of TNF-α-regulated proteins in the nucleus

On the basis of the SILAC results obtained by our time course study, the temporal profile patterns of TNF-α-regulated proteins could be obtained after the ratios were transformed to the log scale (base 2). 547 proteins, which showed a fold change of more than 1.5 and had SILAC results in at least three time points, were chosen to generate the TNF-α response temporal profile patterns. On the basis of the K-means clustering, there were nine different profile patterns and the number of proteins in each profile group is 65 (11.90%), 64 (11.72%), 48 (8.79%), 73 (13.37%), 82 (15.02%), 62 (11.36%), 63 (11.54%), 52 (9.52%) and 38 (6.96%), respectively (Figure 4) (Supplementary information, Table S3).

These known and unknown effectors were clustered into different groups and showed the distinctive temporal

Table 2 Pofile patterns of some proteins associated with TNF-α-induced signaling

IPI Number	0 min	10 min[1]	20 min[1]	30 min[1]	Gene symbol[2]	Subcellular localization[3]	Cluster[4]	References
IPI00790695	NA	–0.53	1.10	–0.57	RPL30 6 kDa protein	NA	1	*Nat Cell Biol* 2004, 6, (2), 97-105
IPI00293426	0	0.23	1.46	0.47	SMARCA4 probable global transcription activator SNF2L4	Cytoplasmic and perinuclear (by similarity)	1	*Mol Cell Biol* 2003, 23, (8), 2749-2761
IPI00604399	0	0.52	0.69	1.06	FANCD2 isoform 2 of fanconi anemia group D2 protein	Nuclear concentrates in nuclear foci during S-phase and upon genotoxic stress	2	*Nat Cell Biol* 2004, 6, (2), 97-105
IPI00003918	0	0.03	0.05	0.68	RPL4 60S ribosomal protein L4	NA	2	*FEBS J* 2005, 272, (15), 3788-3802 *Science* 2001, 292, 1382-1385
IPI00014310	0	0.29	0.16	1.52	CUL1 cullin-1	NA	2	*Biochem Biophys Res Commun* 1999 256, (1), 127-132
IPI00013774	0	0.05	–0.28	0.62	HDAC1 histone deacetylase 1	Nuclear	2	*Mol Cell Biol* 2001, 21, (20), 7065-7077
IPI00289601	0	–0.26	–0.16	0.41	HDAC2 histone deacetylase 2	Nuclear	2	*Mol Cell Biol* 2001, 21, (20), 7065-7077
IPI00301364	0	NA	0.84	0.25	SKP1A isoform 1 of S-phase kinase-associated protein 1A	NA	3	*Ann N Y Acad Sci* 2005, 1053, 356-375
IPI00789457	0	NA	1.00	0.55	KPNA2 karyopherin alpha 2	NA	3	*J Invest Dermatol* 2007, 127, (6), 1456-1464
IPI00025087	0	–0.85	NA	0.36	TP53 isoform 1 of cellular tumor antigen p53	Cytoplasmic and nuclear	3	*Mol Cell* 2007, 26, (1), 75-87 *Clin Cancer Res* 2007, 13, (19), 5680-5691 *Genes Dev* 2006, 20, (2), 225-235
IPI00744507	0	–0.62	NA	–0.43	CSNK2A1 casein kinase II subunit alpha	NA	4	*Cancer Res* 2006, 66, (4), 2242-2249
IPI00798383	0	–0.75	–0.48	–0.42	GNB2L1 26 kDa protein	NA	5	*J Immunol* 2002, 169, 5161–5170
IPI00414676	0	–1.25	–0.80	–0.45	HSP90AB1 heat shock protein HSP 90-beta	Cytoplasmic	5	*Cancer Res* 2007, 1, 67, (19), 9482-9489
IPI00221089	0	–0.97	–0.95	NA	RPS13 40S ribosomal protein S13	NA	5	*Exp Cell Res* 2004, 296, (2), 337-346
IPI00790768	0	–1.86	–1.49	–0.74	YWHAZ 26 kDa protein	NA	5	*J Biochem Mol Biol* 2005, 38, (4), 447-456
IPI00303105	NA	–0.58	–0.00	0.58	SUMO1 small ubiquitin-related modifier 1 precursor	Nuclear; nuclear envelope and nuclear speckles. Also cytoplasmic	5	*J Biol Chem* 1999, 274, (15), 10145-10153
IPI00000816	0	NA	–1.47	–0.59	YWHAE 14-3-3 protein epsilon	Cytoplasmic (By similarity)	5	*J Biol Chem* 2008, 283, (19), 13261-13268

Table 2 Pofile patterns of some proteins associated with TNF-α-induced signaling

IPI Number	0 min	10 min[1]	20 min[1]	30 min[1]	Gene symbol[2]	Subcellular localization[3]	Cluster[4]	References
IPI00299904	0	NA	–0.13	0.69	MCM7 isoform 1 of DNA replication licensing factor MCM7	Nuclear (By similarity)	6	*EMBO J* 2004, 24, 23, (23), 4660-4669 J Biol Chem 2002, 277, (43), 40871-40880
IPI00029695	0	0.61	0.13	0.48	SMARCB1 isoform A of SWI/SNF-related matrix-associated actin-dependent regulator of chromatin subfamily B member 1	Nuclear	6	*Mol Cell Biol* 2003, 23, (8), 2749-2761
IPI00293242	0	0.55	0.35	0.64	GTF2I isoform 2 of general transcription factor II-I	Nuclear and cytoplasmic (Potential)	7	*J Immunol* 2007, 178, (5), 2631-2635
IPI00783837	0	0.74	0.84	0.77	POLR2A DNA-directed RNA polymerase II largest subunit	NA	7	*J Cell Biochem* 2000, 75, (3), 357-368
IPI00783271	0	0.784326	0.391111	0.360187	LRPPRC leucine-rich PPR motif-containing protein	NA	7	*Mol Syst Biol* 2007, 3, 89
IPI00017963	0	0.03	–0.76	–0.12	SNRPD2 small nuclear ribonucleoprotein Sm D2	Nuclear	8	*Nat Biotechnol* 2003, 21, (3), 315-318
IPI00470489	0	0.69	0.75	–2.18	SMARCE1 isoform 2 of SWI/SNF-related matrix-associated actin-dependent regulator of chromatin subfamily E member 1	Nuclear	9	*Mol Cell Biol* 2003, 23, (8), 2749-2761
IPI00641153	0	NA	–0.31	–0.86	GLG1 Golgi apparatus protein 1 precursor	NA	9	*Nat Cell Biol* 2004, 6, (2), 97-105

[1]Protein change was calculated by comparing with zero time point, and then transformed into log scale (base two).
[2, 3]These annotations were obtained from Swiss-Prot database.
[4]The group of profile patterns was revealed by K-means clustering analysis.

patterns of the TNF-α/NF-κB-response pathway. According to our limited survey, many different proteins associated with the TNF-α/NF-κB-signaling pathway were included in particular profile groups (Table 2). For examples, Smarca4 of cluster 1, an important component of an NF-κB-associated complex, which can regulate bfl-1 expression [25], showed an activation profile at the 20 min time point in our results. Histone deacetylase 1 (HDAC1) and histone deacetylase (HDAC2), of cluster 2, have been shown to associate with NF-κB to suppress the expression of NF-κB-regulated genes [26]. As expected, they displayed a significant step-increasing pattern in our experiments. In cluster 3, tumor protein p53 (TP53), a well-known tumor suppressor, showed a temporal pattern of a rapid decrease and an increase afterwards upon TNF-α stimulation. Thus, TP53 levels appear to be inversely associated with NF-κB phospho-p65 [27-29]. These results demonstrate that TP53 may be a negative effector in early nuclear signaling events following TNF-α addition. Protein kinase CK2, in cluster 4, had been reported to suppress various types of tumor necrosis factor-regulated apoptosis [30]. Accordingly, it displayed a decreased profile upon TNF-α stimulation in our study. RACK1, in cluster 5, which is an essential interaction

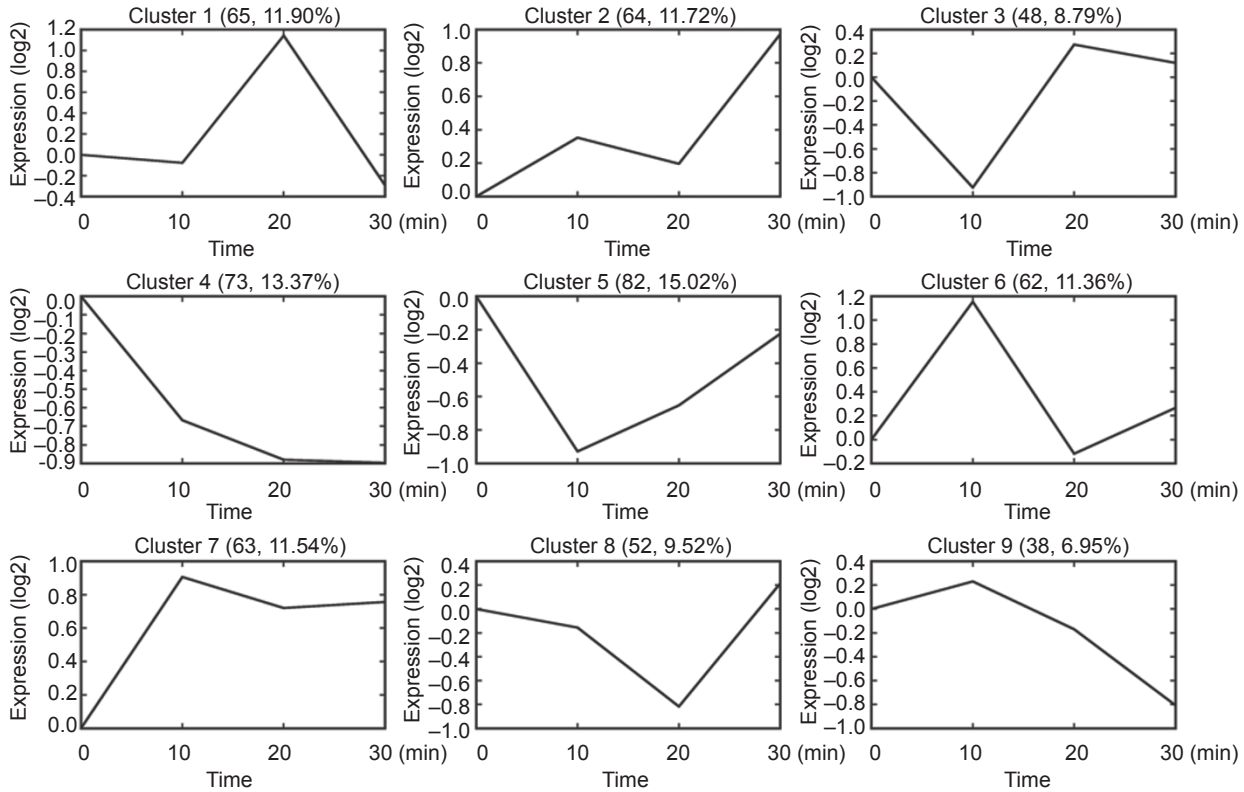

Figure 4 Activation profiles of 547 proteins with a minimum of 1.5-fold change. The 0 min value was used as a basal time point to calculate the protein fold changes in 10 min, 20 min and 30 min. After transformed to the logarithmic scale (base 2), the temporal changed profiles of 547 differentially regulated nuclei-associated proteins were algorithmically subdivided into nine clusters using K-means clustering method. The protein number of each cluster is indicated.

Table 3 The quantitative information of FANCD2

FANCD2			
Fraction	Peptides	Ratio	SD
0 min	—	0.970[1]	0.05[1]
—	AIEEIAGVGVPELINSPK	0.984	—
—	AIEEIAGVGVPELINSPK*	0.977	—
—	LTQHVPLLK*	0.942	—
10 min	—	1.16	0.27
—	IMQLISIAPENLQHDIITSLPEILGDSQHADVGK*	0.97	—
—	VFDSHPVLHVCLK	1.35	—
20 min	—	1.80	0.09
—	LPEYFFENK*	1.73	—
—	LLLGIDILQPAIIK	1.86	—
30 min	—	2.27	—
—	LTQHVPLLK*	2.27	—

[1]Protein ratio and SD were calculated by all quantitative peptides.

* stands for peptides labeled with ^{13}C6-lysine.

partner of p55 TNF receptor [31], showed a quick decrease and slow increase profile. The MCM7, of cluster 6,

which played a key role in DNA replication licensing [32], displayed immediate increase at the 10 min time point, and then was decreased to the basal level. The proteins of cluster 7, such as general transcription factor II (GTFII-I), which plays roles in transcription and signal transduction [33], were increased at the 10 min time point and then were maintained at those levels. This suggests that these proteins may be involved in TNF-α/NF-κB-associated gene transcription. The proteins of cluster 8 include small nuclear ribonucleoprotein D2 [34], which is required for pre-mRNA splicing and small nuclear ribonucleoprotein biogenesis, displayed rapid decreases at the 20 min time point. In cluster 9, proteins such as Golgi apparatus protein 1 (GLG1), which interacts with p52 upon TNF-α stimulation [35], were decreased at the 30 min time point in our study.

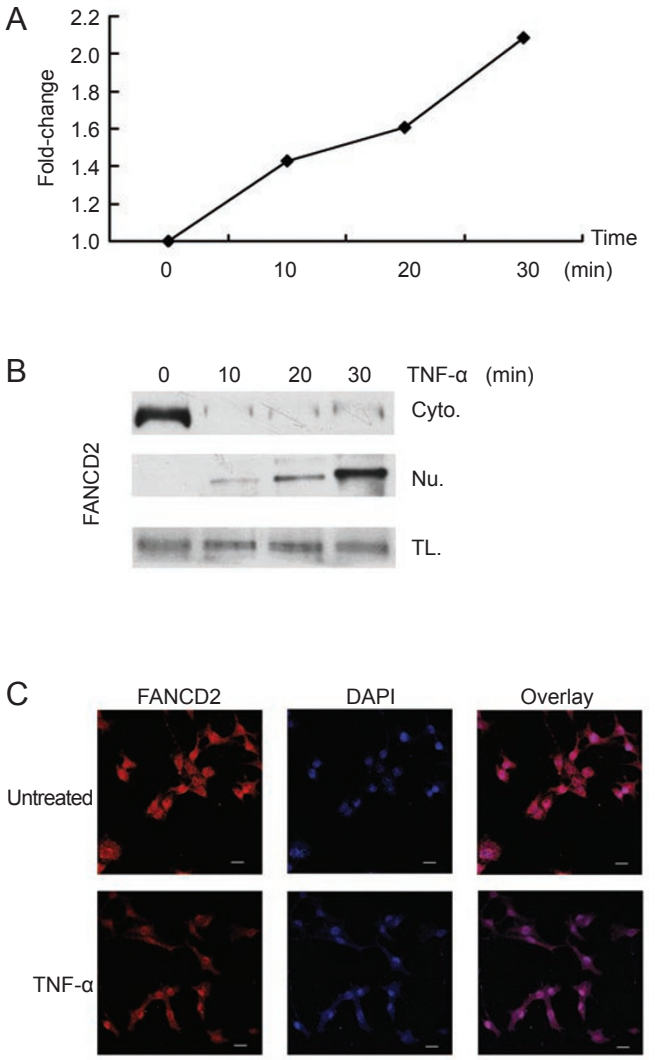

Figure 5 Activation profiles of FANCD2 of TNF-α-induced. **(A)** The kinetic profile of FANCD2. All fold changes were normalized to 0 min. FANCD2 was accumulated in the nucleus upon TNF-α stimulation according to the SILAC results. **(B)** Western blotting analysis of FANCD2. FANCD2 was increased in the nucleus, while reduced in the cytoplasm after the stimulation. **(C)** Confocal micrographs of HEK293 cells that were stimulated with TNF-α for 30 min and those without stimulation. The fixed cells were stained with anti-FANCD2 primary antibody and indodicarbocyanine-tagged secondary antibody (red), and the nuclear dye DAPI (blue). Subcellular distribution of FANCD2 indicated that it was increased upon TNF-α stimulation. Scale bar is 10 mm.

Another interesting protein included in SILAC profiling was Fanconi anemia group D2 protein (FANCD2). Fanconi anemia (FA) is a genetic disease that affects children and adults from all ethnic backgrounds. It is characterized by skeletal anomalies and increased incidence of solid tumors and leukemia, and cellular sensitivity to DNA-damaging agents such as mitomycin C [36]. Some researchers found that the FA complex might facilitate the recruitment of other proteins to maintain genomic integrity in the nucleus [37]. The mono-ubiquitinated form of FANCD2, as the central FA pathway protein, is essential for triggering the FA pathway [38]. Moreover, there is also evidence that FANCD2 interacts specifically with TNFR [35]. In our study, FANCD2 showed a continuous increase upon TNF-α stimulation (Figure 5A, Table 3). To further confirm the changes of FANCD2, western blotting and immunofluorescence analysis were used. The results from western blotting were consistent with the SILAC analysis (Figure 5B). Further, immunofluorescence analysis verified that FANCD2 was increased in the nucleus upon stimulation of TNF-α (Figure 5C). These results suggest that FANCD2 is a new nuclei-effector of TNF-α/NF-κB signaling. Future studies will help to elucidate the function and mechanism of its translocation. Moreover, this suggests that there might be crosstalk between the TNF-α/NF-κB and the FA pathways. Therefore, with the strategy used in this study, not only can known effectors of TNF-α/NF-κB signaling be identified, quantified and sorted, but also new potential effectors can be obtained and annotated according to their temporal nuclear profiles.

Functional analysis on the basis of profile patterns

The differential proteins, with quantitative information in at least three fractions, were also analyzed with Gene Ontology database to examine the preponderance of molecular functions (http://www.ebi.ac.uk/GOA/). Proteins with annotations such as transporter activity (62, 27%), structural molecule activity (49, 22%), transcription regulator activity (46, 21%) and signal transducer activity (28, 13%) were enriched (Figure 6A). In total, 26 proteins were annotated as transcription factor or TF-

associated proteins (Supplementary information, Table S4). Only six of them showed decreasing levels at the 10 min point upon TNF-α stimulation. This suggests that most of these transcription factors were accumulating in the nucleus in response to TNF-α signaling. These regulated proteins may therefore represent TNF-α/ NF-κB-signaling effectors.

Further analysis via K-means clustering of enrichments of KEGG pathways in each profile pattern was adopted to reflect the correlation between the particular profile pattern and the KEGG annotation. Briefly, proteins with a fold change of less than 1.5 upon TNF-α stimulation were selected as the 'tenth cluster'. They likely play non-significant roles in TNF-α/ NF-κB signaling. Proteins of all the nine clusters of temporal profile patterns and the 'tenth cluster' were assigned to 121 pathways by KEGG annotation. Sixty-seven KEGG pathways that had at least three proteins quantified in our study were then used to analyze particular functions represented in each of the profiles. The KEGG pathway enrichments of different profiles were shown via K-means clustering after being normalized and transformed to log scale (Figure 6B) (see method).

The main pathways in cluster 10 were folate biosynthesis, citrate cycle and fatty acid metabolism pathways according to the KEGG annotation. The enrichments of these metabolism pathways were consistent with the character of the fold change of less than 1.5 upon TNF-α stimulation. It verified that the tenth (control) group of proteins were likely not involved in TNF-α/ NF-κB signaling.

Clusters 1 and 2 were classified into the same group according to their KEGG pathway annotations. It is very interesting to note that they had similar quantitative profiles. Proteins in these groups demonstrated increased levels at the 20 or 30 min time points. Calcium signaling, urea cycle and metabolism of amino groups pathways were all over-represented in these groups. For example, Cullin-1 of cluster 1 with the KEGG annotation of calcium-signaling pathway has been reported to play roles in TNF-α/ NF-κB signaling [39, 40].

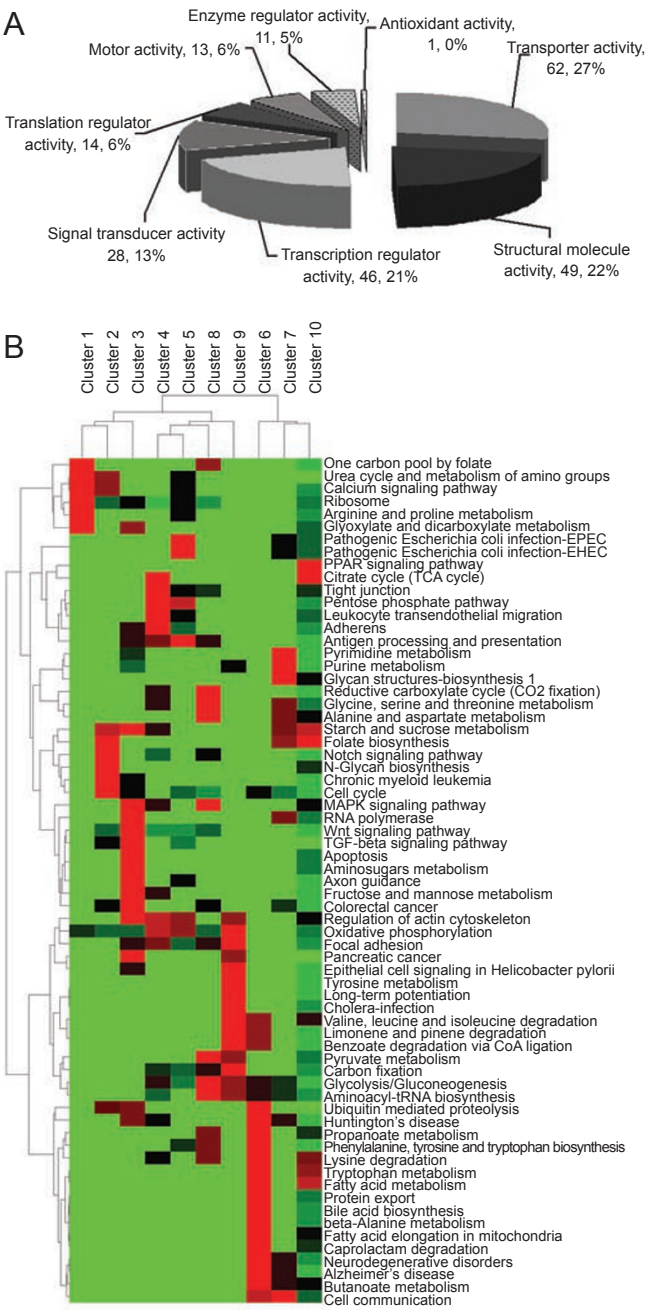

Figure 6 Functional analysis on the basis of the profiles patterns. **(A)** Functional annotation using the Gene Ontology Annotation Database. These proteins, with quantitative information in at least three fractions, were analyzed using the Gene Ontology Annotation Database. GO annotation was retrived for 224 of 547 proteins. Molecular function annotation included transporter activity (62, 27%), structural molecule activity (49, 22%), transcription regulator activity (46, 21%) and signal transducer activity (28, 13%). **(B)** Functional classification using the KEGG pathways annotation. Proteins of each cluster were assigned their biological/metabolic annotation using the KEGG pathways database. Sixty-seven KEGG pathways that had at least three proteins quantified in our study were then used to analyze these protein profiles. This revealed the enrichment of the KEGG pathway related to each profile pattern after calculating, normalizing, transforming to log scale and clustering. These results showed that the profiles with similar pattern were enriched for proteins with similar functions. The horizontal axis shows the different profiles. The longitudinal axis represents the different KEGG pathway. The color reflects the enrichment levels of all these KEGG pathways. Enrichment levels greater than the mean are shaded in red and those below the mean are shaded in green.

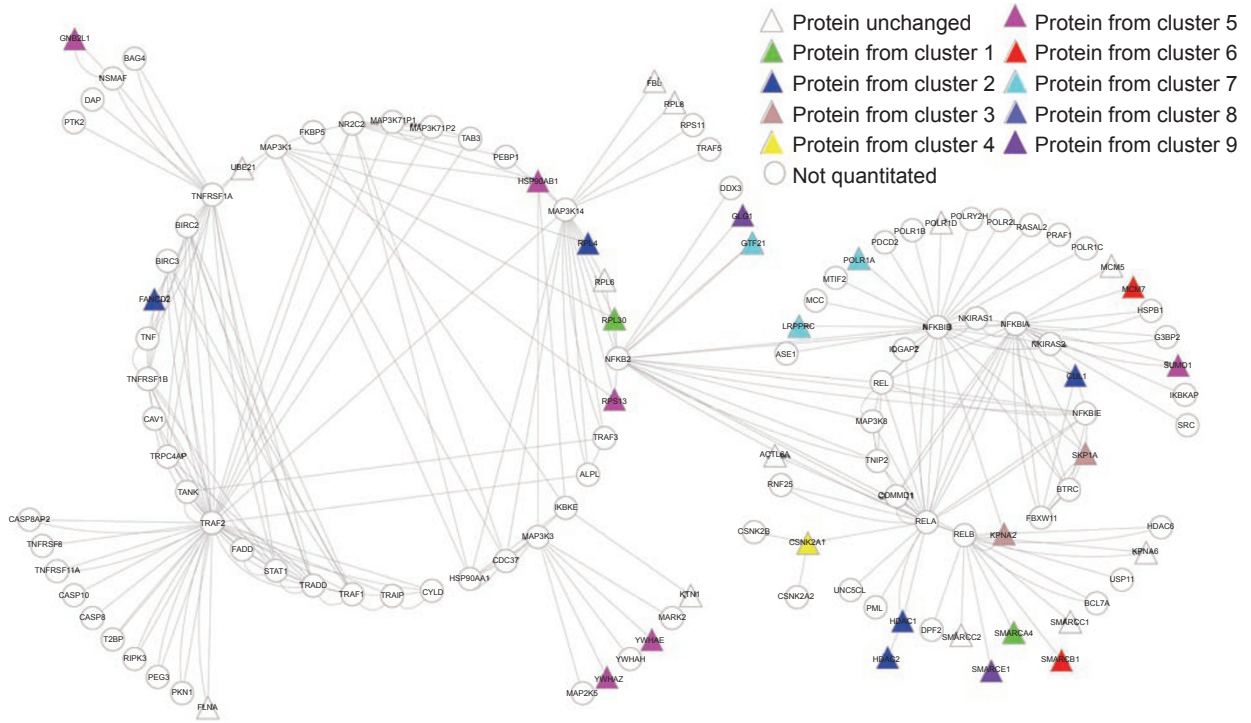

Figure 7 The pathway networks of the TNF-α/NF-κB signaling. Thirty-five proteins with quantitative information were matched in the known TNF-α/NF-κB-signaling pathway according to the HPRD. All the proteins in the TNF-α/NF-κB-signaling pathway are indicated by circles and triangles. The proteins that were quantified in our study are indicated by triangles. Each protein profile is represented in a different color, respectively.

A similar grouping could be drawn for clusters 4 and 5. They showed decreased levels at the early time point, with antigen processing and presentation, oxidative phosphorylation and pentose phosphate pathways being enriched. For example, HSPA8 with the annotation of antigen processing and presentation, the isoform 1 of heat shock cognate 71-kDa protein, is able to translocate rapidly between the cytoplasm and the nucleus. Interestingly, it has been shown that HSP70 members may have a role in regulating TNF signaling by binding to silencer of death domain, a cofactor of TNFR1 [41]. Oxidative phosphorylation and pentose phosphate pathways are also enriched in clusters 4 and 5, suggesting that they may be linked to TNF-α/NF-κB signaling. Interestingly, a resent finding suggests that NF-κB plays an important role in angiotensin II/ROS-induced skeletal muscle insulin resistance in an NAD(P)H oxidase-dependent manner [42].

Clusters 3 and 6 both showed a profile pattern of rapid and brief change. Some pathways, including ubiquitin-mediated proteolysis, which allows NF-κB to translocate to the nucleus and regulate transcription [43], and Huntington's disease pathway reported to be related to TNF-α signaling [44], were enriched in these two clusters.

For cluster 3 alone, some signaling pathways, including MAPK, Wnt and TGF-β signaling pathways, were enriched. These pathways had high physical connections with the TNF-α-signaling pathway [43-45]. Taken together, these results show that the profiles with similar patterns were enriched for proteins with similar functions. This indicates intrinsic correlations between the quantitative profile patterns and protein functions.

Biological network of quantified proteins according to the TNF-α/NF-κB signaling pathway

To further investigate the function of quantified proteins, all proteins with SILAC results in at least three time points were searched in the Human Protein Reference Database (HPRD) (see Method). The results are shown in Figure 7. In total, 35 proteins were matched in the known TNF-α/NF-κB-signaling network, of which 23 proteins had a change of more than 1.5-fold. Furthermore, we compared the quantitative patterns with the physical locations of these proteins in the signaling network. The four most prominent examples were HDAC1 and HDAC2; GTF21, POLR1A and LRPPRC; SKP1A and KPNA2; YWHAE and YWHAZ, which showed that

proteins with similar physical locations in the TNF-α/NF-κB network had the same temporal profile patterns. The SWI/SNF-related matrix-associated actin-dependent regulator chromatin (SMARC) family proteins had different temporal profile patterns upon TNF-α induction. It has been reported that these proteins might be involved in the regulation of a cell death inhibitor upon NF-κB -activating stimuli [25]. Therefore, each of them might have distinct functions in the TNF-α/NF-κB-signaling pathway.

Discussion

In this study, a strategy combining quantitative proteomics, subcellular fractionation and time-course analysis, was developed to delineate the temporal and spatial activation profiles of the TNF-α-signaling pathway. SILAC strategy in combination with high-resolution mass spectrometry had been proved to be a powerful method to generate a panel of differential proteins [23]. Subcellular fractionation provides an attractive method for protein separation. This method has the advantage of reducing the complexity of the samples, and could also help gain proteomics information for analysis of components and functions of different subcellular structures [46-48]. On the basis of time-course analysis, dynamic changes in protein levels can be obtained. In this study, the temporal and spatial profile patterns of 547 nuclei-associated TNF-α-regulated proteins were delineated. Moreover, many previously unknown effectors of TNF-α/NF-κB signaling were identified, quantitated and sorted into differential activation profiles.

Subcellular distribution analysis of cellular proteins is one of the major tasks of proteomics. Furthermore, protein nucleocytoplasmic shuttling is often a key regulator of different cellular processes. These shuttling behaviors help to compartmentalize specific protein functions to different organelles in response to cytokines [16]. The cytokine-induced nuclear import and export of signaling proteins have been shown to be essential in various biological systems [17, 18]. In this study, we investigated the early dynamic changes of nuclei-associated proteins following TNF-α signaling and provided a dynamic and global view of such changes. Moreover, spatial changes in protein localization following signal transduction can be measured by our method, as shown here for FANCD2. By employing such a combined strategy, we can not only measure the levels of signaling-associated proteins by quantitative proteomics, but also delineate the dynamic spatial changes of them. Further work analyzing additional subcellular fractions (nucleus, cytosol, mitochondria, membrane, golgi, ER and so on) may help obtain a more complete and dynamic readout of proteome changes in response to TNF-α signaling.

Signal transduction is a key field of study in modern biological research. Although large-scale high-throughput experimental techniques have greatly increased our knowledge of signal transduction pathways [10-15], our understanding of the signaling process is nevertheless incomplete. Our study here represents the thus far largest-scale, dynamic and systematic analysis of TNF-α/NF-κB signaling.

Materials and Methods

Chemicals and regents

Stable isotope-containing amino acids ^{13}C6-lysine and ^{12}C6-lysine were purchased from Cambridge Isotope Labs (Andover, MA, USA). The RPMI1640 medium deficient in L-lysine was a custom medium preparation from Chemicon (Temecula, CA, USA). ProteoExtract™ subcellular proteome extraction kit was purchased from Merck (Darmstadt, Germany). Antibodies were obtained from Santa Cruz Biotechnology. Sequencing Grade Modified Trypsin was obtained from Promega (Madison, WI, USA). ACN for high-performance liquid chromatography (HPLC) grade was obtained from Fisher (Fair Lawn, NJ, USA). Other chemicals employed were purchased from Sigma (St Louis, MO, USA).

Stable isotope labeling with amino acids in cell culture

HEK293 cells were cultured in RPMI1640 medium containing ^{12}C6-lysine ('light') or ^{13}C6-lysine ('heavy') supplemented with 10% dialyzed fetal bovine serum plus antibiotics [15]. A detailed protocol is available at http://www.silac.org. Briefly, HEK293 cells were adapted to grow in the isotope-containing media supplemented with dialyzed serum and maintained for six passages to ensure a complete replacement, prior to the addition of ligand. The labeled cells were stimulated with 20 ng/ml TNF-α for 10 min, 20 min or 30 min. The unstimulated cells were considered as the zero time point.

Subcellular fractionation

Treated and untreated cells were immediately harvested, and subcellular components were separated by ProteoExtract™ subcellular proteome extraction kit (Calbiochem, Merck, Germany). According to the protocol supplied in the kit, the nuclear, cytosolic, organelle/membrane and cytoskeletal fraction were obtained.

Protein preparation and trypsin digestion

Nuclear fractions were dialyzed, lyophilized and resolubilized in a reducing solution (6 M urea, 4%CHAPS, 65 mM DTT and 40 mM Tris) [49]. Protein quantitation was performed using the Bradford protein assay, and equal amounts of protein in the four 'heavy' fractions were mixed as a standard. The four 'light' fractions and such a standard were mixed at a protein concentration ratio of 1:1. These protein mixtures were subsequently digested by trypsin [49].

Western blotting procedures

After SDS-PAGE separation, proteins were transferred to nitro-

cellulose membranes. The membrane was first blocked with Net Gelatin (150 mM NaCl, 5 mM EDTA, 50 mM pH 7.5, 0.05% Triton X-100 and 0.25% Gelatin) and then incubated with appropriate primary and HRP-conjugated secondary antibodies. Antibody labeling was visualized using ECL reagent (Pierce) according to the manufacturer's instructions. Image analysis of immunoblots was performed using QuantityOne software (Bio-Rad).

Immunofluorescence analysis

HEK293 cells grown on glass coverslips were either treated with TNF-α for 30 min or untreated, and then fixed in 4% paraformaldehyde for 20 min. Fixed cells were incubated with blocking buffer and then immunofluorescent staining was performed with appropriate primary and secondary antibodies. Images were taken using Leica DM RE confocal microscopy.

Continuous pH elution SCX-RP-LC-MS/MS analysis

A surveyor liquid chromatography system (Thermo Finnigan, San Jose, CA, USA) consisting of a degasser, 2 MS Pumps and an autosampler were used. The separation conditions and columns utilized were: (1) a SCX column (320 μm × 100 mm, Column Technology Inc., CA, USA); (2) two C18 trap columns (RP, 300 μm × 5 mm, Agilent Technologies, USA); (3) an analytical C18 column (RP, 75 μm × 150 mm, Column Technology Inc.) and (4) 15 μm (internal diameter) non-coated SilicaTip™ PicoTip™ nanospray emitter (New Objective, Woburn, MA, USA). We applied a pH-dependent elution system for peptide mixture separation using strong cation exchange HPLC. The solvents used were A (pH 2.5) and B (pH 8.5). The pH gradient buffer was obtained from Column Technology, Inc.).

Three hundred micrograms of the peptide mixtures were dissolved in 80 μl of pH 2.5 buffer A, and then loaded onto the SCX column at a flow rate of 3 μl/min after the split. A continuous pH gradient was constituted of a mixture of buffer A (pH 2.5) and buffer B (pH 8.5). The final gradient was maintained as 100% buffer B (pH 8.5) and, in total, ten fractions were obtained. The C18 trap columns were used to bind peptides eluted from SCX by pH gradient. When a reverse-phase gradient was run in trap column 1, peptides eluted from the SCX column by the following pH gradient were loaded onto trap column 2 and vice versa [50].

The solvents for reverse-phased HPLC were 0.1% formic acid (v/v) aqueous (A) and 0.1% formic acid (v/v) acetonitrile (B). The entire RP gradient run was from 0% to 35% of mobile phase B in 165 min. The flow rate was 140 μl/min before the splitting and 250 nl/min after the splitting. The whole chromatography process was fully automated.

A linear ion trap/Orbitrap (LTQ-Orbitrap) hybrid mass spectrometer (Thermo Finnigan) equipped with an NSI nanospray source was operated in data-dependent mode to automatically switch between MS and MS/MS acquisition with an ion transfer capillary of 200 ºC and NSI voltage of 1.85 kv. Normalized collision energy was 35.0. The mass spectrometer was set so that one full MS scan was acquired in the Orbitrap parallel to (or following) 10 MS2 scans in the linear ion trap on the 10 most intense ions from the full MS spectrum with the following Dynamic Exclusion™ settings: repeat count was 2, repeat duration was 30 s, exclusion duration was 90 s. The resolving power of the Orbitrap mass analyzer was set at 100 000 ($m/\Delta m$ 50% at m/z 400) for the precursor ion scans.

Database search and quantitative analysis

All the dta files were created using Bioworks 3.2, and they were automatically searched against the IPI human database (ipi.HUMAN.v3.28.REVERSED.fasta) using the TurboSEQUEST program. One missing trypsin cleavage site was allowed [51]. Carbamidomethylation was searched as a fixed modification and isotope-labeled lysine (+6.00 Da) was allowed as a variable modification [15]. All output results were combined using an in-house software named BuildSummary with the 0.01 FPR (False-Positive Rate) filter [52]. To eliminate redundancy, the proteins were classified to a protein group if the same peptides were assigned to multiple proteins after false peptides were filtered. For the quantitative analysis, only those lysine-containing peptides that can be assigned to single protein groups were sent to an in-house SysQuant program.

Preprocessing of the quantitation data and K-means clustering

Due to the systematic error of the Bradford protein assay, it could be necessary to normalize the SILAC results. By using the labeled peptide ratio (Ratio=Total Peptide $hits_{light}$/Total Peptide $hits_{heavy}$) in each fraction, the bias of such quantitation was reduced. After preprocessing, K-means clustering approach was employed to analyze the differential expression [53]. Before the clustering analysis, protein ratios were transformed to the log scale (base 2), which would convert the distribution of relative abundance values for all quantitative proteins into a more symmetric and almost normal pattern [54]. We selected the protein groups that had a 1.5-fold change and had quantitative information in at least three fractions. And from each protein group only one representative protein was selected. The number of clusters was set as nine to classify the data set after tested. The Cluster 3.0 freeware software package was used (http://bonsai.ims.u-tokyo.ac.jp/~mdehoon/software/cluster/software.htm). Repeated (10-100) K-means clustering of proteins was based on Pearson correlation coefficient of their expression profiles (ratios in three time points). The prototype (mean profile) was then plotted using a python 2D plotting library—Matplotlib (http://matplotlib.sourceforge.net/) [15]. The clustered data profiles were visualized in pseudocolor heat map format using the TreeView software package (http://jtreeview.sourceforge.net).

Function analysis of all the clusters according to the Kyoto Encyclopedia of Genes and Genomes (KEGG) database

Proteins with a fold change of less than 1.5 upon TNF-α stimulation in the present study were selected as the 'tenth cluster'. Proteins of all the nine clusters according to the temporal profile pattern and the 'tenth cluster' were searched against KEGG database [55]. This was used to assign biological/metabolic annotation. All the ten clusters were annotated with protein numbers in different KEGG pathways. The KEGG pathway enrichments of different profiles were demonstrated after calculating, normalizing, transforming to log scale and clustering. The method for the normalization and clustering was similar to preprocessing of the quantitation data and K-means clustering.

Network modeling on the basis of Human Protein Reference Database

The TNF-α signaling pathway networks were obtained from HPRD (http://www.hprd.org/). The signaling networks were visualized by using Cytoscape [56].

Acknowledgment

We would like to thank Dr Ian Scott (Department of Molecular Genetics, University of Toronto), Dr Chengjian Tu (Vanderbilt Medical Center, Vanderbilt University) and Ya-Wen Tian (Key Laboratory of Systems Biology, Shanghai Institutes for Biological Sciences) for critical reading of the manuscript. This work was supported by the National Natural Science Foundation of China (30425021, 30521005), Basic Research Foundation (2006CB910700), CAS Project (KSCX2-YW-R-106, KSCX1-YW-02) and High-technology Project (2007AA02Z334).

References

1 MacEwan DJ. TNF ligands and receptors—a matter of life and death. *Br J Pharmacol* 2002; **135**:855-875.
2 Wajant H, Grell M, Scheurich P. TNF receptor associated factors in cytokine signaling. *Cytokine Growth Factor Rev* 1999; **10**:15-26.
3 Karin M. Nuclear factor-kappaB in cancer development and progression. *Nature* 2006; **441**:431-436.
4 Ghosh S, May MJ, Kopp EB. NF-kappa B and Rel proteins: evolutionarily conserved mediators of immune responses. *Annu Rev Immunol* 1998; **16**:225-260.
5 Chan FK, Chun HJ, Zheng L, *et al*. A domain in TNF receptors that mediates ligand-independent receptor assembly and signaling. *Science* 2000; **288**:2351-2354.
6 Yang J, Lin Y, Guo Z, *et al*. The essential role of MEKK3 in TNF-induced NF-kappaB activation. *Nat Immunol* 2001; **2**:620-624.
7 Wertz IE, O'Rourke KM, Zhou H, *et al*. De-ubiquitination and ubiquitin ligase domains of A20 downregulate NF-kappaB signalling. *Nature* 2004; **430**:694-699.
8 Ong SE, Blagoev B, Kratchmarova I, *et al*. Stable isotope labeling by amino acids in cell culture, SILAC, as a simple and accurate approach to expression proteomics. *Mol Cell Proteomics* 2002; **1**:376-386.
9 Mann M. Functional and quantitative proteomics using SILAC. *Nat Rev Mol Cell Biol* 2006; **7**:952-958.
10 Hinsby AM, Olsen JV, Bennett KL, Mann M. Signaling initiated by overexpression of the fibroblast growth factor receptor-1 investigated by mass spectrometry. *Mol Cell Proteomics* 2003; **2**:29-36.
11 Lim YP, Diong LS, Qi R, Druker BJ, Epstein RJ. Phosphoproteomic fingerprinting of epidermal growth factor signaling and anticancer drug action in human tumor cells. *Mol Cancer Ther* 2003; **2**:1369-1377.
12 Stasyk T, Dubrovska A, Lomnytska M, *et al*. Phosphoproteome profiling of transforming growth factor (TGF)-beta signaling: abrogation of TGFbeta1-dependent phosphorylation of transcription factor-II-I (TFII-I) enhances cooperation of TFII-I and Smad3 in transcription. *Mol Biol Cell* 2005; **16**:4765-4780.
13 Wang Y, Li R, Du D, *et al*. Proteomic analysis reveals novel molecules involved in insulin signaling pathway. *J Proteome Res* 2006; **5**:846-855.
14 Zheng H, Hu P, Quinn DF, Wang YK. Phosphotyrosine proteomic study of interferon alpha signaling pathway using a combination of immunoprecipitation and immobilized metal affinity chromatography. *Mol Cell Proteomics* 2005; **4**:721-730.
15 Tang LY, Deng N, Wang LS, *et al*. Quantitative phosphoproteome profiling of Wnt3a-mediated signaling network: indicating the involvement of ribonucleoside-diphosphate reductase M2 subunit phosphorylation at residue serine 20 in canonical Wnt signal transduction. *Mol Cell Proteomics* 2007; **6**:1952-1967.
16 Saint Fleur S, Fujii H. Cytokine-induced nuclear translocation of signaling proteins and their analysis using the inducible translocation trap system. *Cytokine* 2008; **41**:187-197.
17 Brivanlou AH, Darnell JE Jr. Signal transduction and the control of gene expression. *Science* 2002; **295**:813-818.
18 Cyert MS. Regulation of nuclear localization during signaling. *J Biol Chem* 2001; **276**:20805-20808.
19 Gerondakis S, Grossmann M, Nakamura Y, Pohl T, Grumont R. Genetic approaches in mice to understand Rel/NF-kappaB and IkappaB function: transgenics and knockouts. *Oncogene* 1999; **18**:6888-6895.
20 Hoffmann A, Levchenko A, Scott ML, Baltimore D. The IkappaB-NF-kappaB signaling module: temporal control and selective gene activation. *Science* 2002; **298**:1241-1245.
21 Hinsby AM, Kiemer L, Karlberg EO, *et al*. A wiring of the human nucleolus. *Mol Cell* 2006; **22**:285-295.
22 Graham JM. Isolation of nuclei and nuclear membranes from animal tissues. *Curr Protoc Cell Biol*. New York: John Wiley & Sons, Inc, 2001: Unit 3.10.
23 Kruger M, Kratchmarova I, Blagoev B, *et al*. Dissection of the insulin signaling pathway via quantitative phosphoproteomics. *Proc Natl Acad Sci USA* 2008; **105**:2451-2456.
24 Cantin GT, Venable JD, Cociorva D, Yates JR, 3rd. Quantitative phosphoproteomic analysis of the tumor necrosis factor pathway. *J Proteome Res* 2006; **5**:127-134.
25 Edelstein LC, Lagos L, Simmons M, Tirumalai H, Gelinas C. NF-kappa B-dependent assembly of an enhanceosome-like complex on the promoter region of apoptosis inhibitor Bfl-1/A1. *Mol Cell Biol* 2003; **23**:2749-2761.
26 Ashburner BP, Westerheide SD, Baldwin AS Jr. The p65 (RelA) subunit of NF-kappaB interacts with the histone deacetylase (HDAC) corepressors HDAC1 and HDAC2 to negatively regulate gene expression. *Mol Cell Biol* 2001; **21**:7065-7077.
27 Huang WC, Ju TK, Hung MC, Chen CC. Phosphorylation of CBP by IKKalpha promotes cell growth by switching the binding preference of CBP from p53 to NF-kappaB. *Mol Cell* 2007; **26**:75-87.
28 Lee TL, Yang XP, Yan B, *et al*. A novel nuclear factor-kappaB gene signature is differentially expressed in head and neck squamous cell carcinomas in association with TP53 status. *Clin Cancer Res* 2007; **13**:5680-5691.
29 Kashatus D, Cogswell P, Baldwin AS. Expression of the Bcl-3 proto-oncogene suppresses p53 activation. *Genes Dev* 2006; **20**:225-235.
30 Wang G, Ahmad KA, Ahmed K. Role of protein kinase CK2 in the regulation of tumor necrosis factor-related apoptosis inducing ligand-induced apoptosis in prostate cancer cells. *Cancer Res* 2006; **66**:2242-2249.
31 Tcherkasowa AE, Adam-Klages S, Kruse ML, *et al*. Interaction with factor associated with neutral sphingomyelinase

activation, a WD motif-containing protein, identifies receptor for activated C-kinase 1 as a novel component of the signaling pathways of the p55 TNF receptor. *J Immunol* 2002; **169**:5161-5170.

32 Yanagi K, Mizuno T, You Z, Hanaoka F. Mouse geminin inhibits not only Cdt1-MCM6 interactions but also a novel intrinsic Cdt1 DNA binding activity. *J Biol Chem* 2002; **277**:40871-40880.

33 Ashworth T, Roy AL. Cutting Edge: TFII-I controls B cell proliferation via regulating NF-kappaB. *J Immunol* 2007; **178**:2631-2635.

34 Blagoev B, Kratchmarova I, Ong SE, *et al*. A proteomics strategy to elucidate functional protein-protein interactions applied to EGF signaling. *Nat Biotechnol* 2003; **21**:315-318.

35 Bouwmeester T, Bauch A, Ruffner H, *et al*. A physical and functional map of the human TNF-alpha/NF-kappa B signal transduction pathway. *Nat Cell Biol* 2004; **6**:97-105.

36 Kinzler KW, Vogelstein B. Cancer-susceptibility genes. Gatekeepers and caretakers. *Nature* 1997; **386**:761, 763.

37 de Winter JP, van der Weel L, de Groot J, *et al*. The Fanconi anemia protein FANCF forms a nuclear complex with FANCA, FANCC and FANCG. *Hum Mol Genet* 2000; **9**:2665-2674.

38 Sobeck A, Stone S, Hoatlin ME. DNA structure-induced recruitment and activation of the Fanconi anemia pathway protein FANCD2. *Mol Cell Biol* 2007; **27**:4283-4292.

39 Suzuki H, Chiba T, Kobayashi M, *et al*. IkappaBalpha ubiquitination is catalyzed by an SCF-like complex containing Skp1, cullin-1, and two F-box/WD40-repeat proteins, beta-TrCP1 and betaTrCP2. *Biochem Biophys Res Commun* 1999; **256**:127-132.

40 Lyapina S, Cope G, Shevchenko A, *et al*. Promotion of NEDD-CUL1 conjugate cleavage by COP9 signalosome. *Science* 2001; **292**:1382-1385.

41 Miki K, Eddy EM. Tumor necrosis factor receptor 1 is an ATPase regulated by silencer of death domain. *Mol Cell Biol* 2002; **22**:2536-2543.

42 Wei Y, Sowers JR, Clark SE, *et al*. Angiotensin II-induced skeletal muscle insulin resistance mediated by NF-kappaB activation via NADPH oxidase. *Am J Physiol Endocrinol Metab* 2008; **294**:E345-E351.

43 Yoshimura A, Mori H, Ohishi M, Aki D, Hanada T. Negative regulation of cytokine signaling influences inflammation. *Curr Opin Immunol* 2003; **15**:704-708.

44 Bubici C, Papa S, Dean K, Franzoso G. Mutual cross-talk between reactive oxygen species and nuclear factor-kappa B: molecular basis and biological significance. *Oncogene* 2006; **25**:6731-6748.

45 Ohazama A, Sharpe PT. TNF signalling in tooth development. *Curr Opin Genet Dev* 2004; **14**:513-519.

46 Oh P, Li Y, Yu J, *et al*. Subtractive proteomic mapping of the endothelial surface in lung and solid tumours for tissue-specific therapy. *Nature* 2004; **429**:629-635.

47 Zhao Y, Zhang W, White MA. Capillary high-performance liquid chromatography/mass spectrometric analysis of proteins from affinity-purified plasma membrane. *Anal Chem* 2003; **75**:3751-3757.

48 Mootha VK, Bunkenborg J, Olsen JV, *et al*. Integrated analysis of protein composition, tissue diversity, and gene regulation in mouse mitochondria. *Cell* 2003; **115**:629-640.

49 Jiang XS, Zhou H, Zhang L, *et al*. A high-throughput approach for subcellular proteome: identification of rat liver proteins using subcellular fractionation coupled with two-dimensional liquid chromatography tandem mass spectrometry and bioinformatic analysis. *Mol Cell Proteomics* 2004; **3**:441-455.

50 Zhou H, Dai J, Sheng QH, *et al*. A fully automated 2-D LC-MS method utilizing online continuous pH and RP gradients for global proteome analysis. *Electrophoresis* 2007; **28**:4311-4319.

51 Dai J, Jin WH, Sheng QH, *et al*. Protein phosphorylation and expression profiling by Yin-yang multidimensional liquid chromatography (Yin-yang MDLC) mass spectrometry. *J Proteome Res* 2007; 6:250-262.

52 Tabb DL, McDonald WH, Yates JR, 3rd. DTASelect and Contrast: tools for assembling and comparing protein identifications from shotgun proteomics. *J Proteome Res* 2002; **1**:21-26.

53 Hartigan JA, Wong MA. A K-means clustering algorithm. *Appl Stat* 1979; **28**:100-108.

54 Callister SJ, Barry RC, Adkins JN, *et al*. Normalization approaches for removing systematic biases associated with mass spectrometry and label-free proteomics. *J Proteome Res* 2006; **5**:277-286.

55 Kanehisa M, Goto S. KEGG: kyoto encyclopedia of genes and genomes. *Nucleic Acids Res* 2000; **28**:27-30.

56 Shannon P, Markiel A, Ozier O, *et al*. Cytoscape: a software environment for integrated models of biomolecular interaction networks. *Genome Res* 2003; **13**:2498-2504

(**Supplementary information** is linked to the online version of the paper on the Cell Research website.)